

Structure and energetics of giant fullerenes: An order- N molecular-dynamics study

Satoshi Itoh

Central Research Laboratory, Hitachi, Ltd., Tokyo 185, Japan
and Department of Physics, University of Illinois at Urbana-Champaign, Urbana, Illinois 61801

Pablo Ordejón*

Department of Physics, University of Illinois at Urbana-Champaign, Urbana, Illinois 61801
and Materials Research Laboratory, University of Illinois at Urbana-Champaign, Urbana, Illinois 61801

David A. Drabold

Department of Physics and Astronomy, Condensed Matter and Surface Science Program, Ohio University, Athens, Ohio 45701-2979

Richard M. Martin

Department of Physics, University of Illinois at Urbana-Champaign, Urbana, Illinois 61801
and Materials Research Laboratory, University of Illinois at Urbana-Champaign, Urbana, Illinois 61801

(Received 26 July 1995)

We present a molecular-dynamics study of the energetics and structures of very large carbon cage clusters, which has been performed using tight-binding methods, both empirical and *ab initio*. The use of an order- N scheme, which provides the solution of the electronic problem with an effort proportional to the size of the system, allowed us to study clusters with up to 3840 atoms. We have considered clusters with spherical and with toroidal topology, and systematically find that spherical clusters have lower energy than toroidal clusters of the same size. However, the toroidal C_{360} and larger clusters have lower energy per atom than the fullerene C_{60} . Concerning the spherical fullerenes, we show that, in all cases, their minimum energy shape is markedly polyhedral rather than spherical. The clusters present nearly flat faces between each three contiguous protruding pentagon sites. The surfaces are nevertheless smooth, without sharp edges in the lines joining the pentagons, which would be present in a perfect truncated icosahedron. We also discuss the energetics of the clusters as a function of their size, and the validity of different functional forms proposed in the literature.

I. INTRODUCTION

After the discovery of the fullerene C_{60} ,¹ many kinds of carbon structures have been observed experimentally.² For instance, higher fullerenes, crystals of C_{60} molecules, multi-shell fullerenes,³ single wall tubes,⁴ polymerization of C_{60} molecules in the solids,⁵ and so on. In all these materials, the configuration of the polygonal network of carbon bonds and the atomic coordinates constitute important pieces of information for finding out the formation mechanism and the structural properties. Since a precise experimental determination of these is often very difficult, the theoretical evaluation of the geometrical parameters is of paramount importance for an understanding of the properties of these materials. This has become particularly evident in the study of very large, single-shell fullerene cages. The observation by Ugarte³ of multishell fullerenes formed by many concentric fullerene balls of different sizes one inside the other, has triggered interest in the study of large single-shell fullerenes, as a preliminary step to understand the observed extremely spherical shapes of the multishell fullerenes.

Since isolated, large defect free single-shell fullerenes have not been observed experimentally, a theoretical investigation of these forms of carbon is important, and has been undertaken from different points of view. Theoretical work based on elasticity theory,^{6,7} as well as calculations using empirical interatomic potentials,^{6,8,9} seemed to establish that

the most stable form of large single-shell fullerenes is markedly polyhedrally faceted instead of perfectly spherical. Therefore, one conclusion drawn from these studies is that the reason for the multishell fullerenes being spherical is not the stability of the spherical single shells, and that the inter-shell (van der Waals) interaction, or kinetic processes, are determinant of the experimentally observed structures. Recent *ab initio* calculations^{10,11} on large single-shell fullerenes have challenged this view, however, indicating that nearly spherical clusters may be more stable than polyhedral ones. With these results, the idea that the spherical structure of multishell clusters may be due to an intrinsic stability of the spherical single-shell fullerenes has been retaken.¹²

Another important piece of information, which theoretical atomistic simulations can provide and that is difficult to extract from the experiments, is the relative stability of each of the different clusters as a function of its shape and size, and compared to other forms of carbon (like graphite), or to the same class of materials, with different geometrical parameters. This is the case concerning the relative stability of fullerenes with different topologies, like spherical and toroidal clusters. Also, the specific way in which the energy of a spherical cluster approaches that of an infinite graphite plane as its size increases has been the subject of several studies.^{6,7,13}

Most of the theoretical work done so far on the energetics and structure of giant fullerenes have been based on macro-

scopic theories (like elasticity theory), or in classical microscopic theories (empirical interatomic potentials). The application of quantum-mechanical electronic structure methods has been reduced to relatively small clusters (up to C_{240}) until very recently. This is naturally, due to the intense numerical effort involved in this type of calculation, and the N^3 scaling of this effort with the size of the system, which makes the calculations nonpractical for a systems larger than a very few hundred atoms. In the past two years, however, several techniques have emerged that allow the calculation of the energy and the dynamics of large systems from the electronic structure, with an effort proportional to the size of the system.¹⁴ These so-called order- N methods have allowed the study of systems with thousands of atoms, and are, therefore, ideal for realistic computations on complex materials like the large fullerenes. One of these methods was used by Yang and co-workers for the *ab initio* study of single-shell fullerenes mentioned above.^{10,11}

In this work, we have applied one of these recently developed order- N methods to study the shape, structure, and energetics of giant fullerenes. In order to have a more robust and complete picture, we have used two different electronic structure models: an empirical tight-binding method (in which the interaction parameters are fitted to experimental and *ab initio* information of diamond and graphite), and a first principles approach based in the local density approximation (LDA). The purpose of this study is fourfold: (i) To study the validity and accuracy of the order- N approach to treat this important kind of material, and develop efficient techniques to accelerate the solution of the electronic problem in these systems. We will show that the order- N algorithm used here provides excellent accuracy in these systems, compared to standard methods like diagonalization. (ii) To calculate the most stable shape of large single-shell fullerenes, to help decide if sphericity is preferred or the shapes tend to be polyhedral. The results of our calculation support the conclusion that, for all the studied clusters larger than C_{60} , the shapes are markedly polyhedral, with nearly flat facets and protruding pentagonal sites. (iii) To study the energetics of the clusters as a function of their size, and compare with those of toroidal clusters to check the relative stability. We will show that the fullerenes are always more stable than the toroidal clusters of similar size, but that toroidal clusters larger than C_{360} have lower energy than the C_{60} spherical fullerene. (iv) To make use of the results obtained for the energetics of the clusters used to test the validity of several formulas proposed in the literature for the dependencies of the cluster energy versus size, which were derived using macroscopic or empirical theories.

The paper is organized as follows. Section II contains a summary of the order- N algorithm used, and the two electronic structures models that we have utilized. Section III describes strategies to apply efficiently the order- N techniques to these systems, and shows the typical accuracies obtained with the method. In Sec. IV, we describe our results for the most stable shapes of large fullerenes, from C_{60} to C_{3840} , whereas in Sec. V we study the energetics of the clusters and the dependence with the cluster size. Finally, Sec. VI contains the conclusions of this work.

II. METHODOLOGY

The objective of the present work is to study very large clusters, with sizes up to several thousand atoms. For these sizes, the use of traditional techniques to solve the electronic problem is obviously out of the question. The reason is the N^3 scaling of the required computational effort with the number of electrons in the system. Recently, however, a number of methods¹⁴ have been developed in which the numerical load scales only linearly with the size of the system (therefore referred to as order- N methods). In this work, we have applied one of these order- N schemes, the one developed by Ordejón *et al.*¹⁵ and by Mauri *et al.*¹⁶ We refer the reader to Ref. 14 for a detailed description of the method. Here, we will just outline the main ideas involved: (i) the use of an energy functional which does not require orthogonalization of the electronic wave functions, and (ii) a description of the occupied electronic states in terms of Wannier-like localized wave functions (LWF's), which are truncated beyond a certain cutoff, instead of eigenvectors.

The band structure energy functional

$$\tilde{E}_{\text{bs}}[\{\psi_i\}] = 2 \left[\sum_{i=1}^N H_{ii} - \sum_{i,j=1}^N H_{ji}(S_{ij} - \delta_{ij}) \right] \quad (1)$$

is defined for $2N$ electrons, in terms of N doubly occupied states $|\psi_i\rangle$, $i=1, \dots, N$, where $S_{ij} = \langle \psi_i | \psi_j \rangle$, $H_{ij} = \langle \psi_i | \hat{H} | \psi_j \rangle$, and the factor 2 is for the spin. It can be shown that the minimization of \tilde{E}_{bs} with respect to any arbitrary set of occupied states $|\psi_i\rangle$, which are not restricted to be orthogonal, leads to the exact ground state band structure energy of the system. Moreover, the set of states that minimize \tilde{E}_{bs} is an orthogonal set. Therefore, the ground state band structure energy E_{bs} can be computed minimizing \tilde{E}_{bs} without imposing any orthogonality constraint, using a conjugate gradients algorithm.

In order to achieve the linear scaling, we notice that the set of functions $|\psi_i\rangle$ defining the ground state is not unique, since any unitary transformation of these states has the same energy. In particular, we can describe the ground state by means of orthonormal localized wave functions centered at different positions. Since, similarly to the Wannier functions, the LWF's decay rapidly with distance,¹⁷ we can truncate them beyond a certain cutoff radius from the center as an approximation. The combination of the unconstrained energy functional and the LWF's produces a linear scaling algorithm.

Our calculations are based on the tight-binding scheme. We have used two methods, which are very different in nature (one being empirical, the other *ab initio*). The first is an empirical tight-binding (ETB) model for total energies of carbon systems developed by Xu *et al.*¹⁸ The model assumes a basis of four orbitals per C atom (one s and 3 p 's), which are orthogonal (i.e., the overlap between orbitals in different atoms is taken as zero, regardless of the interatomic distance). The total energy in this scheme is computed as

$$E_{\text{tot}} = E_{\text{bs}} + E_{\text{rep}}, \quad (2)$$

where E_{bs} is the band structure energy, and E_{rep} is a repulsion term which is defined as a sum of pairwise potentials between atoms. Both the Hamiltonian matrix elements and the

repulsion potential are parametrized, and fitted as a function of the interatomic distance, so as to reproduce experimental and first principles information for different phases of carbon. This ETB scheme has proven useful for the study of fullerenes and other forms of carbon. However, the empirical nature of the method and the far from obvious transferability of the Hamiltonian, makes it useful to compare the results obtained with a more accurate and less *ad hoc* method. For this reason, we have also used the *ab initio* tight-binding (AITB) method of Sankey and Niklewski.¹⁹ This method is based on the LDA approximation, and uses the non-self-consistent Harris functional, together with a minimal basis of localized, atomic like orbitals to describe the valence electrons, and pseudopotentials to eliminate the core electrons from the calculation. It is, therefore, a nonparametrized method, which has been extensively tested with excellent results for systems containing carbon, as well as other elements. In this method, the total energy takes the same form as Eq. (2), where the band structure energy is computed from the nonparametrized Hamiltonian, and the repulsive term includes the ion-ion interactions plus correction terms to account for overcounting of the Hartree and exchange correlation energy in E_{bs} . Since the basis used is nonorthogonal, the overlap matrix must be taken into account when computing the eigenvalues of \hat{H} .

III. LOCALIZED WAVE FUNCTION

As mentioned in Sec. II, the order- N method employed in this work^{15,16} is based on the use of localized wave functions, which are truncated, instead of the extended eigenstates of the Hamiltonian.¹⁴ There are many possible schemes to assign the parameters defining each LWF's (such as the position of the center of each function and their radial cutoff), like assigning two LWF's to the position of each C atom, so that a total of $2N$ are defined. However, a more sophisticated approach that takes into account the chemistry and local bonding of the material can be much more advantageous from the computational point of view. In this section, we describe the strategy that we have followed in this work to define and build the LWF's.

The carbon cage clusters that are considered here have the following properties: (i) they contain only carbon atoms, (ii) there are no dangling bonds, and (iii) each atom holds covalent bonds with three neighbors. These systems, therefore, are formed by a σ -bonded network of atoms with sp^2 hybridization. Since there are four valence electrons in the $2s$ and $2p$ orbitals of each carbon atom, three of them form σ bonds with an electron from each of the three neighbor atoms, respectively. The remaining one electron contributes to the π orbitals of the cluster. Thus, for a cluster with N carbon atoms and $4N$ electrons, $3N$ electrons occupy $3N/2$ bonds of a σ type and N electrons occupy $N/2$ bonds of a π type.

The structure of the network of σ and π bonds suggest a natural and efficient way of defining the localized functions for the order- N calculation, their center of localization, and the initial guess to start the band energy minimization. We define $3N/2$ LWF's corresponding to σ -type orbitals, and $N/2$ corresponding to π -type orbitals. As an initial guess for the minimization, we use the bonding combination of sp^2

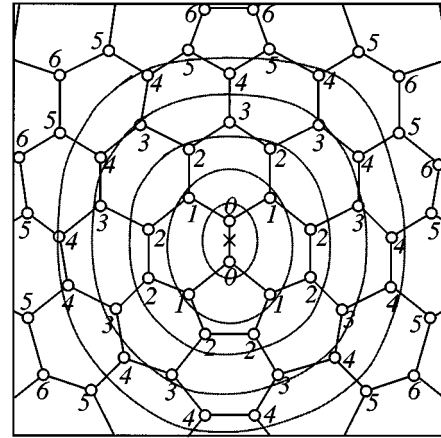


FIG. 1. Schematic view of the areas enclosed by different values of the cutoff N_c from the center of a bond (marked with a cross) for the definition of a LWF.

orbitals forming the σ bonds, and of p_{\perp} orbitals for the π bonds. Each of the σ functions is centered at one of the $3N/2$ bonds of the cage network. The choice for the location of the π LWF's is more subtle, since there is only one π function per each pair of atoms, and, therefore, the choice of the center of localization is not unique. The distribution of centers must be homogeneous, in order to optimize the calculation and to ensure local charge neutrality when truncated LWF's are used. The scheme that we have used here is suggested by the double-single bond structure of C_{60} : the bonds joining different pentagons are short in length, and, therefore, contain a π bond, whereas the bonds shared by a pentagon and a hexagon are long, single σ bonds. We can, therefore, assign a π LWF to each of the $N/2$ double bonds of C_{60} . For larger spherical or toroidal clusters, where the structure of double and single bonds is lost (as in graphite), we use the same construction scheme: we start assigning π functions to each of the bonds going outwards radially from the pentagons, and continue assigning π functions to bonds in alternating positions. It is easy to see that, using this procedure, the structures are covered with $N/2$ bonds of π type, in such a way that each atom forms part of just one of these bonds, ensuring that the distribution is homogeneous.

Once the centers of the localization of the LWF's are assigned as described in the previous paragraph, a localization radius must be chosen for the LWF's. Usually, a real space cutoff R_c , defined by a geometrical distance, is used to determine which atoms are included in each of the localized functions.¹⁴ Instead, for the systems under consideration, we find it useful to use a different definition. We define the distance between an atom and the center of the LWF as the minimum integer number of bonds between the atom and the bond in which the LWF is centered. The atom is then included in the LWF if this distance is smaller than a cutoff N_c . Figure 1 shows the area enclosed by several values of N_c , from the center of a particular bond. We see that for $N_c=0$, there are just two atoms in each LWF, for $N_c=1$, six atoms are in the range, and so on. This definition has the advantage that the number of atoms within the cutoff depends only on the topology of the bonds, and not on the

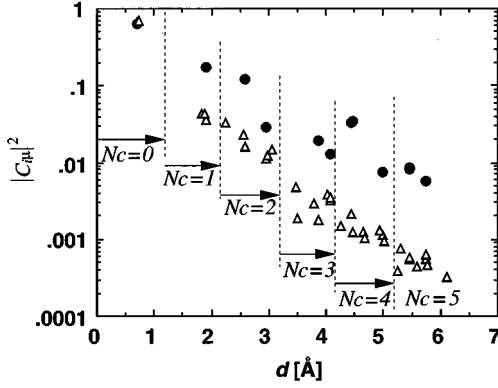


FIG. 2. Decay of the localized wave function of C_{60} . σ functions (white triangles) decay much faster than π functions (black circles).

curvature of the structure, and, therefore, on the size of the cluster.

The choice of the localization range N_c depends on the particular system under consideration. For systems with a large gap, the LWF's decay very rapidly (exponentially¹⁷), so the value of N_c can be chosen to be small. For systems with a small gap, or for metals, the decay is much slower (a power law in the case of metals¹⁷), and larger values of N_c must be used to preserve accuracy. Figure 2 shows the decay of the LWF's versus the distance from their center, for the spherical cluster C_{60} , obtained with the ETB method with an infinite cutoff radius. The distances corresponding to different values of the cutoff N_c are also shown in Fig. 2. As expected, the LWF's decay exponentially with the distance. However, the decay is much faster for the σ functions than for the π functions. This characteristic is common to all carbon clusters considered, as well as to graphite. The reason is that the states in the vicinity of the energy gap are primarily π states, so their localization is weaker than for σ states. Therefore, increasing the cutoff for σ orbitals will not provide much improvement to the accuracy, while increasing the cutoff for the π orbitals will have a much larger effect. There is obviously no reason to maintain the same cutoff for both types of LWF's, so we have determined the optimum values of N_c^σ and N_c^π . We show, in Fig. 3, the total energies of icosahedral C_{240} versus the computational time per minimization iteration for several combinations of the cutoff distances N_c^σ and N_c^π . In this figure, the lower points correspond to higher accuracy, and the points more on the left correspond to faster computations. The increase of N_c^π from 2-4 for the same value of $N_c^\sigma=2$ improves the accuracy, while not increasing the computational time much. On the other hand, increasing N_c^σ from 2-4 for the same distance $N_c^\pi=4$ does not change the accuracy significantly, but increases the computational time drastically. To quantify our results, the total energies of icosahedral C_{60} and C_{240} calculated with the ETB model, using different combinations of cutoff distances, are listed in Table I. $N_c^\sigma=2$ and $N_c^\pi=4$ is the most optimum set of cutoff values, providing excellent accuracy for both clusters. These results hold for the AITB method as well. In what follows, and unless specified otherwise, the results presented

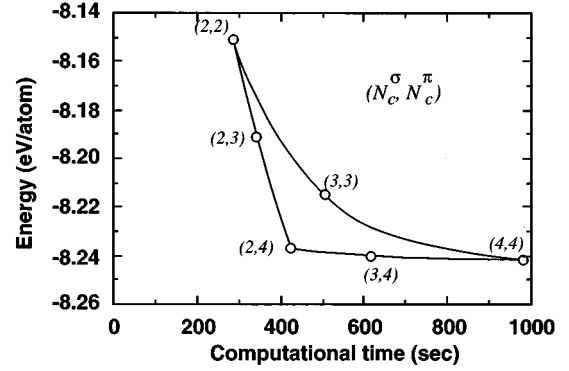


FIG. 3. Energy of icosahedral C_{240} for several different cutoff distances N_c^σ and N_c^π . The horizontal axis indicates CPU time for one iteration of energy minimization on a SUN/Sparc-ipc workstation.

have been obtained using these cutoff values.

The error in the order- N solution is larger for the C_{240} cluster than for C_{60} . This is due to the closing of the gap from 1.6 eV in C_{60} to 1.1 eV in C_{240} . Increasing the cluster size further (and, therefore, decreasing the gap value) does not seem to further degrade the accuracy in a significant manner. For instance, in a graphite plane (where the gap is zero), the error for $N_c^\sigma=2$ and $N_c^\pi=4$ is 0.024 eV/atom for ETB and 0.053 eV/atom for AITB (the total energy per atom for the order- N solution is -8.362 eV/atom, compared to -8.386 eV/atom for the exact solution in the ETB model, and -157.848 eV/atom versus -157.900 eV/atom for the AITB model).

IV. SHAPES OF FULLERENES

We have used molecular-dynamics techniques to obtain minimum energy structures of the spherical and toroidal fullerenes. In general, we used structures optimized with Stillinger-Weber (SW) potentials²⁰ as initial coordinates. These were then relaxed using our order- N method with either ETB or AITB Hamiltonians. The relaxations were performed using a dynamical quenching algorithm, either with Newtonian or with first-order equations of motion. The optimization continues until the maximum force is smaller than 0.04 eV/Å.²¹ This procedure does not warrant that the obtained structures are the absolute minimum energy structures, but rather local minima. However, further annealing and quenching did not produce structures with lower energies. We are, therefore, confident that our structures represent an

TABLE I. Total energies per atom (in eV) for icosahedral C_{60} and C_{240} calculated with several combinations of cutoff distances N_c^σ and N_c^π , for the ETB model. In parentheses, we show the error percentage, with respect to the exact (∞, ∞) results.

(N_c^σ, N_c^π)	C_{60}	C_{240}
(2,2)	-7.942 (0.82%)	-8.151 (1.4 %)
(3,3)	-7.991 (0.21%)	-8.215 (0.58%)
(4,4)	-8.000 (0.10%)	-8.242 (0.25%)
(2,4)	-7.995 (0.16%)	-8.237 (0.31%)
(∞, ∞)	-8.008	-8.263

TABLE II. Bond lengths (in Å) of spherical C_{60} .

	Double bond	Single bond
Present (ETB)	1.396	1.458
Present (AITB)	1.400	1.449
SW ^a	1.592	1.604
TB ^b	1.396	1.458
LDA ^c	1.40	1.45
NMR ^d	1.40 ± 0.015	1.45 ± 0.015

^aReference 29.^bReference 18.^cReference 22.^dReference 23.

accurate representation of the ground states for each cluster.

In order to establish the accuracy of the ETB and AITB Hamiltonians and of the order- N algorithm used in this work, we analyze first the results for the spherical fullerene C_{60} . Table II shows the lengths of single and double bonds of spherical C_{60} obtained in our calculations, compared to other calculations and with experimental data. Our results from ETB and AITB are in excellent agreement with those of LDA calculations²² and NMR measurement.²³ In particular, the results of the ETB Hamiltonian are exactly the same as those obtained by Xu *et al.*,¹⁸ using the same Hamiltonian, but no order- N approximation. Therefore, our order- N method provides excellent accuracy for structural properties.

The next spherical cluster that we have studied is C_{240} . This cluster has been considered by several authors, which concluded that the structure is polyhedrally faceted, with a significant deviation from sphericity. Yoshida and Osawa⁸ and Dunlap *et al.*²⁴ reported structures, derived from two different empirical potentials, which were practically identical, with a standard deviation from a sphere of 0.17 Å. Adams²⁵ also found a faceted structure using the same AITB model as the one used in this work. Recently, however, York, Lu, and Yang¹⁰ reported results of a lower energy almost spherical structure for C_{240} . The calculations are based on a model

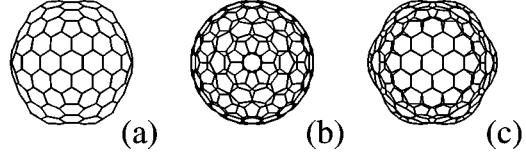


FIG. 4. Optimized C_{240} cluster, viewed along three different axes: (a) a twofold rotation axis, (b) a fivefold rotation axis, and (c) a threefold axis.

closely related with the AITB method used here, combined with an order- N algorithm developed by Yang.²⁶ In their study, York *et al.* considered several different geometries as initial configurations, and relaxed the structures following a simplex algorithm (preserving the icosahedral symmetry). Two of these structures were spherical (denoted “sph1” and “sph2”), and three of them were faceted (“fac1,” “fac2,” and “fac4”). These relaxations yielded two different structures: an almost spherical structure “ S_{York} ” with lower energy, and a polyhedral structure “ P_{York} ” higher in energy by 0.07 eV/atom. The parameters defining the initial and final structures and their energies as calculated by York *et al.* are summarized in Table III. The main result of their calculation is that the spherical clusters always have lower energy than polyhedral clusters, in contrast with the results of others. In order to shed some light in this issue, we have used our AITB model with the order- N formulation to relax the C_{240} cluster. We start with the coordinates from a relaxation of the structure with SW potentials, and follow a dynamical quenching algorithm described above. From this calculations, we obtain the structure that is shown in Fig. 4. The parameters defining the structure are shown in the last row of Table III. We see that the optimized structure for the C_{240} cluster is significantly faceted, with a standard deviation from sphericity of 0.153 Å. This seems to confirm the results of empirical potentials calculations, and is in disagreement with the findings of York *et al.* In order to check that our structural minimization was indeed converged to the most

TABLE III. Geometric parameters (in Å) and energies per atom (in eV, referred to that of a graphite sheet) for different forms of the spherical C_{240} obtained with the AITB method. For the energies of the clusters, we show the results of the AITB Hamiltonian obtained both with exact diagonalization (under E_{exact}) and with our order- N formulation (under $E_{O(N)}$). For comparison, we show the order- N results of York *et al.* (under E_{York}).

Morphology	Bonds (b_1, b_2, b_3, b_4, b_5) ^a	Radii (r_1, r_2, r_3) ^a	$\bar{r}(\sigma)$ ^b	$E_{O(N)}$	E_{exact}	E_{York}
sph1 ^c	(1.44, 1.43, 1.44, 1.43, 1.44)	(7.12, 7.12, 7.12)	7.120 (0.000)	0.185	0.169	0.128
sph2 ^c	(1.43, 1.44, 1.43, 1.43, 1.44)	(7.12, 7.12, 7.12)	7.120 (0.000)	0.194	0.176	0.128
fac1 ^c	(1.48, 1.44, 1.48, 1.44, 1.48)	(7.03, 7.42, 6.97)	7.098 (0.188)	0.502	0.488	0.248
fac2 ^c	(1.47, 1.43, 1.47, 1.43, 1.47)	(7.63, 7.21, 6.75)	7.085 (0.367)	0.241	0.232	0.278
fac4 ^c	(1.45, 1.40, 1.47, 1.45, 1.46)	(7.49, 7.19, 7.05)	7.195 (0.180)	0.141	0.131	0.208
S_{York} ^c	(1.43, 1.43, 1.45, 1.42, 1.44)	(7.01, 7.13, 7.14)	7.106 (0.056)	0.210	0.195	0.108
P_{York} ^c	(1.43, 1.42, 1.51, 1.47, 1.46)	(7.66, 7.19, 7.07)	7.247 (0.244)	0.212	0.200	0.178
YO ^d	(1.43, 1.38, 1.45, 1.42, 1.43)	(7.36, 7.06, 6.92)	7.065 (0.180)	0.122	0.111	
This work	(1.42, 1.38, 1.45, 1.42, 1.43)	(7.32, 7.06, 6.94)	7.065 (0.153)	0.120	0.108	

^aInequivalent bonds and radii. See Ref. 10 for the definition.^bAverage radius and standard deviation (in parentheses).^cOptimized structures obtained by York *et al.* (Ref. 10).^dOptimized structure obtained by Yoshida and Osawa (Ref. 8).

TABLE IV. Average (\bar{r}) and standard deviation (σ) of radii and planarity $\phi = 360^\circ - (\theta_1 + \theta_2 + \theta_3)$ around pentagons in the spherical clusters. SW, ETB, and AITB indicate results obtained using Stillinger-Weber potentials, the empirical tight-binding method, and the *ab initio* tight-binding method, respectively.

	$\bar{r}(\sigma, \sigma/\bar{r})$			ϕ		
	SW	ETB	AITB	SW	ETB	AITB
C ₂₄₀	7.86 (0.29, 0.037)	7.06 (0.17, 0.025)	7.06 (0.15, 0.021)	13.16	8.92	7.88
C ₅₄₀	11.75 (0.46, 0.040)	10.53 (0.36, 0.034)	10.53 (0.35, 0.033)	13.13	9.92	9.19
C ₉₆₀	15.64 (0.64, 0.041)	14.02 (0.53, 0.038)	14.01 (0.52, 0.037)	13.11	9.95	9.28
C ₂₁₆₀	21.65 (1.18, 0.054)	20.95 (0.82, 0.039)	20.95 (0.82, 0.039)	13.10	10.05	9.31
C ₃₈₄₀	29.13 (1.68, 0.058)	27.95 (1.08, 0.039)		13.07	10.05	

stable structure for the C₂₄₀ cluster, we have also calculated the energy of all the structures considered by York *et al.* The results are also shown in Table III. We see that our optimized structure is significantly lower in energy than the rest of the structures considered, including the minima found by York *et al.* Only the polyhedral structure proposed by Yoshida and Osawa,⁸ which is very similar to our optimized structure, is energetically comparable to it. It is interesting to see that even the ordering of energies is very different for our results and those of York *et al.* In order to check that our order- N results are genuine, and not an artifact of the order- N approximation, we have computed the exact energy (within the AITB Hamiltonian), using diagonalization for all the structures. We see in Table III that the energy ordering is the same as the one obtained in the order- N calculation (in particular, our optimized structure is still the minimum energy structure). The difference between the exact and the order- N results seems to be a shift of about 0.01–0.02 eV. Most of this error comes from the fact that the accuracy of the order- N method for graphite is slightly different than for the C₂₄₀ fullerenes. We conclude, therefore, that our order- N results are accurate, and describe properly the energetics of the C₂₄₀ cluster, within the AITB model utilized. The results obtained using the ETB model are essentially the same, as discussed in the next paragraph, which indicates that the preference towards a polyhedral shape is a robust result, since it does not depend on the particular Hamiltonian utilized. The source of discrepancy between our results and those of York *et al.* is unknown at this point. Since these authors use a Hamiltonian model, which is rather similar to the AITB model used by us, one would expect the same qualitative results.

We have performed similar calculations for larger spherical fullerenes, using both the ETB and the AITB models. We have considered the clusters C₂₄₀, C₅₄₀, C₉₆₀, C₂₁₆₀, and C₃₈₄₀. For all the cases (except for C₃₈₄₀, which was computed only with the ETB model) minimum energy structures were obtained using both Hamiltonians. The general result is that, for all sizes and with both models, the clusters are markedly polyhedral, with a larger deviation from sphericity for the larger clusters. We show in Table IV the average radius and the standard deviation from sphericity for all the clusters, computed for the optimum geometries obtained with SW potentials and with the ETB and AITB models. The agreement between ETB and AITB is remarkable, and confirms that the ETB model of Xu *et al.* is an excellent Hamiltonian for these systems. Figure 5 shows a scheme of the structures optimized with the ETB model, from C₂₄₀ to

C₃₈₄₀. We see that, although the clusters are polyhedral, with flat facets between the protruding pentagons, the edges joining the pentagonal sites are not sharp, but rounded, in order to minimize the bending energy. Our calculations confirm the results obtained with empirical potentials by Maiti *et al.*,⁹ who predicted polyhedral shapes for the large fullerenes. Also Witten and Li⁷ predicted shapes similar to those obtained by us, based on elasticity arguments. They, in fact, predicted that the elastic energy would be concentrated in the round edges regions, whereas the flat faces would be similar to graphite. These results emerge from an analysis of the balance between the energy cost of bending at the edges, and the elastic energy that represents any deviation from the flat graphite structure: bond stretching energy is stored in the planes for any deviation from the perfect polyhedral shape; the balance between this energy and the energy cost of bending at the edges determines the shape of the clusters. Witten and Lu predicted that the clusters would have flat facets (to minimize the elastic energy), but soft, round edges (to minimize the bending energy). Our results agree with these predictions.

Recently, Lu and Yang¹¹ performed a study of large fullerene balls, similar to the one reported here. They used the same method as the one used by York *et al.* for the study of C₂₄₀, and obtained qualitatively similar results for the larger clusters: large, isolated clusters were predicted to be spherical, in contrast with our findings. Based on their results, Lu and Yang explained the experimental observation of

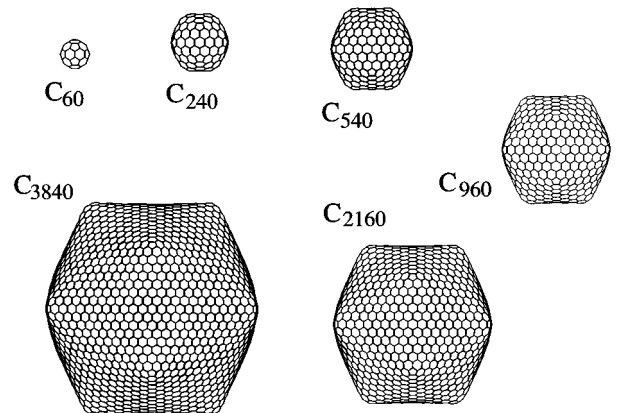


FIG. 5. Nonperspective view of the optimized structures of large fullerene balls, obtained with the ETB model, and viewed from a twofold symmetry axis.

spherical, multishell fullerenes,³ as a consequence of the stability of spherical single-shell fullerenes. Our results contradict these arguments, and suggest that there must be a different mechanism (like intershell interactions) to explain the stability of spherical multishell fullerenes.

The results of Table IV indicate that, as a general result, the optimum structures of large fullerene balls are polyhedral, with a larger deviation from sphericity for larger sizes. The ratio of deviation to the average radius of the cluster saturates, however, for about 2160 atoms. This seems to indicate that these clusters have reached the asymptotic large size regime, and increasing the size roughly preserves the shape of the cluster, with rescaled dimensions. Another measure of the nonsphericity is provided by the amount of nonplanarity of the surface at the pentagonal sites. In the polyhedral structures, the pentagons are protruding, and, therefore, there is a large deviation from planarity at those sites. Following York *et al.*,¹⁰ we define the planarity at an atom by the angle $\phi \equiv 360^\circ - (\theta_1 + \theta_2 + \theta_3)$, where θ_1 , θ_2 , and θ_3 are the angles formed by the three σ bonds between the atom and its three nearest neighbors. Therefore, $\phi = 0^\circ$ for a planar site. We show, in Table IV, the results of the planarity angle ϕ for atoms in the pentagons, for all the clusters from C_{240} to C_{3840} . We see that, as observed in the deviation from sphericity, the planarity at pentagonal sites approaches a constant value for the larger clusters, again indicating that the asymptotic region has been reached. It is interesting to observe that the quantum-mechanical results, both with the ETB and the AITB models, predict a behavior, which is qualitatively different from the results of Stillinger-Weber potentials. Whereas the increase in the ratio σ/\bar{r} is observed in all cases, the SW potentials predict a decrease in the nonplanarity at pentagonal sites with the cluster size, whereas the ETB and AITB models predict an increase for larger sizes. This indicates that, although empirical models can be appropriate for describing the main features of the clusters, the details are far from accurately described.

We have also initiated a study of the shapes and energies of toroidal carbon clusters. Itoh and co-workers²⁷⁻²⁹ proposed several possibilities of toroidal clusters, using molecular dynamics with SW potentials²⁰ determined for graphite by Abraham and Batra.³⁰ The negative curvature is obtained by a combination of pentagons (in the outer face of the torus) and heptagons (in the inner face). Very similar structures have been found experimentally,³¹ although multilayered and larger than the theoretically proposed structures. We have relaxed the structure of toroidal C_{240} , C_{360} , and C_{960} , both with the ETB and AITB models. The tendency of the surface curvature for the toroidal clusters is very similar to that for the spherical clusters. Only the regions around the pentagons are protrusive and the planarity ϕ around the pentagons reaches the same value as that of spherical clusters. An extensive study of the shapes of these and larger toroidal clusters is underway, and will be published elsewhere.³²

V. ENERGIES OF FULLERENES

We have investigated the total energy of the relaxed fullerenes, as a function of their size. Figure 6 shows the total energy per atom relative to that of monolayer graphite. We show the results for the spherical and the toroidal

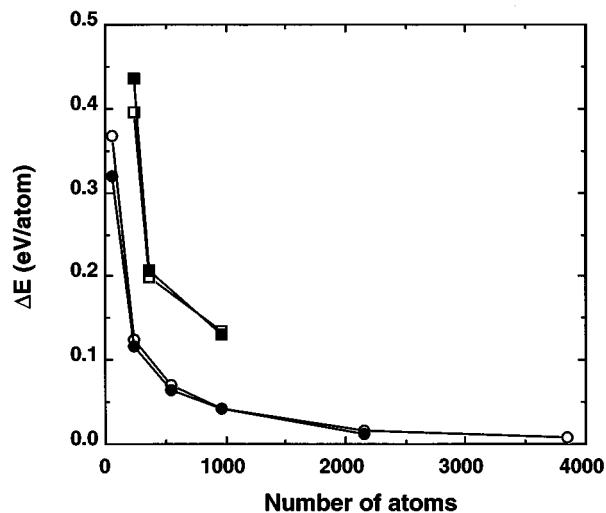


FIG. 6. Total energy per atom for spherical (circles) and toroidal (squares) carbon cage clusters against the total number of carbon atoms. The open symbols correspond to the results of the ETB model, and the black symbols to the AITB model.

fullerenes, obtained both with the ETB and AITB models. It is worth mentioning that there is remarkable agreement between these two models for all the cases studied, which confirms that the simple ETB model produces a very reliable description of this kind of carbon materials. Table V shows the values for the relaxed spherical fullerenes, with both Hamiltonian models. The results of Fig. 6 show that the spherical fullerenes are more stable than the toroidal fullerenes of the same size. The toroidal C_{240} is still less stable than icosahedral C_{60} , although larger toroidal clusters are more stable than C_{60} . These results agree with previous calculations done in the tight-binding approximation³³ and with *ab initio* self-consistent field calculations.³⁴

As shown in Fig. 6, the energies of the fullerenes approach the energy of graphite, as expected since the local bonding in the fullerenes is very close to that in graphite, and increasing the size of the cluster should make the energy approach the value of a graphite plane. Moreover, as we have seen, in the large fullerenes the clusters are faceted, and large portions of the surface are flat, so that the resemblance to graphite is ever more pronounced. However, the detailed way in which the energy approaches that of graphite is an interesting issue, which has attracted some interest in the past. Several studies were made to derive expressions for this dependence, reaching different functional forms depending

TABLE V. Total energies relative to the graphite monolayer (in eV/atom).

N	ETB	AITB
60	0.3674	0.3279
240	0.1253	0.1204
540	0.0693	0.0726
960	0.0430	0.0511
2160	0.0166	0.0221
3840	0.0084	-

TABLE VI. Fits of calculated energies to functional forms E_1-E_4 . $E(n)$ refers to the number of data points used: $n=3$ refers to a fit only to C_{960} , C_{2160} , and C_{3840} ; $n=6$ refers to these plus C_{60} , C_{240} , and C_{540} . The resulting fits are in units of eV/atom.

	$E_1(3)$	$E_1(6)$	$E_2(3)$	$E_2(6)$	$E_3(3)$	$E_3(6)$	$E_4(3)$	$E_4(6)$
A	30.71	34.81	86.83	-3.06	12.20	11.28	138.6	9.06
B	10254	-766.8	-6.62	6.13			1.18	0.783
χ^2	1.1×10^{-7}	1.6×10^{-4}	4.6×10^{-9}	5.2×10^{-5}	4.1×10^{-5}	2.3×10^{-4}	2.4×10^{-10}	7.9×10^{-5}

on which assumptions were made about the shape and about the most important contributions to the energy. We are aware of three theories for the evolution of fullerene energy as a function of n .^{6,7,13} The assumption of spherical symmetry and consideration of fullerene topology, leads to an asymptotic functional form:¹³

$$E_1(n) = A/n + B/n^2, \quad (3)$$

for some coefficients A and B . Such a form should be expected to be most successful for perfectly spherical fullerenes, since there is no assumption of faceting in the model. Adams *et al.*¹³ used *ab initio* local basis methods to obtain energies for many fullerenes, with up to 240 atoms, and found Eq. (3) to provide a satisfactory fit to their energies, even for nonicosahedral balls. A second model is due to Tersoff,⁶ who has used elasticity theory to compute asymptotic estimates of the energies. His functional form is

$$E_2(n) = A/n + B \ln(n)/n. \quad (4)$$

Tersoff also found good agreement with data generated from his empirical potential for carbon.³⁵ Witten and Li⁷ have correctly predicted polyhedral structures and performed calculations, which suggest that the deviation of energy from graphite is mostly due to strain at facet faces. Since the energy is predicted to scale like the ball radius $R^{1/3}$, the relative energy should behave like

$$E_3(n) = A/n^{5/6}. \quad (5)$$

For completeness, we will also considered the general single power-law decay:

$$E_4(n) = A/n^B. \quad (6)$$

To attempt to gauge the suitability of these predictions, we have performed least squares fits³⁶ of our energies to each of E_1-E_4 . Since the energies obtained with the ETB and AITB models are quite similar (see Table V), we used those from the ETB model to perform the fits. We did two sets of fits, one including the energies of all (six) fullerenes, and another with just the largest three (C_{960} , C_{2160} , and C_{3840}). The latter calculations were performed to obtain better estimates of the asymptotic behavior of the energy. We also report the squared deviation of the fits:

$$\chi^2 = \sum_{i=1}^{N_p} (E^i - E_i)^2, \quad (7)$$

where E^i is our calculated energy, E_i is the value of the fitting function (one of E_1-E_4), and N_p is the number of points (3 or 6) used in the fitting. The result of these fits is summarized in Table VI. It is clear that all the proposed

forms offer an acceptable fit to the data of Table V. The best overall fit for $N_p=6$ is from the Tersoff form, E_2 , though it should be emphasized that the other functional forms are also quite reasonable. What is perhaps of greater interest is the case of fits to the three largest fullerenes. The best fit is for a simple power-law with $N^{-1.176}$ scaling. This result provides some evidence that a simple power-law decay is the appropriate asymptotic form, but with only three points, this view must be held with caution. Certainly the Tersoff and Adams forms cannot be discarded. Each of these forms has two free parameters adjusted to minimize χ^2 . The form of Witten and Li has only one parameter, and also fits reasonably well. In Fig. 7, we plot our computed energies, and a pair of illustrative fits. As the plot is doubly logarithmic, its near linearity suggests that a power law is reasonable, particularly for the last three points, as we have seen.

Unfortunately it is difficult to indicate a strong preference for one of these models over the others. For one thing, the values of the fitting parameters are *very* sensitive to the number of points used (not surprising with such a small number of points). In addition, the basic nature of the functional forms is so similar, especially with two free parameters, that a simple judgment does not seem to be possible. In the presence of more data, and a detailed understanding of the nature of errors in the calculations, the methods of Bayesian model selection³⁷ would be appropriate to assign probabilities to each model. This would enable a quantitative measure of the trade-off between the higher χ^2 of Witten and Li⁷ and the smaller number of parameters being fit, for example.

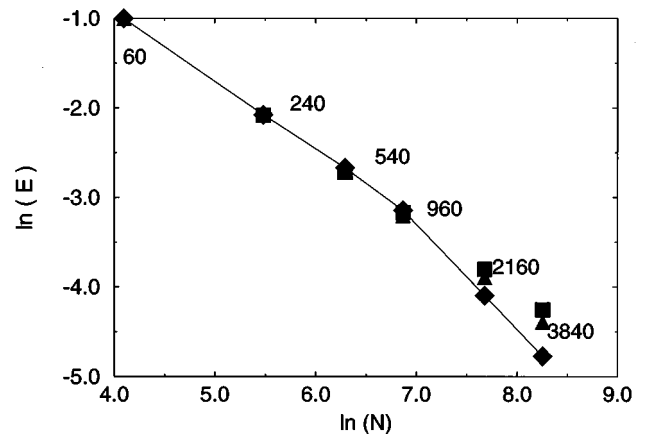


FIG. 7. Log-log plot of cluster size (N) versus relative energy. Diamonds are the result of the present calculation, and the line is a guide to the eye. Two fits to the energies are shown. Squares depict a power law [$E_4(6)$], and triangles depict the Tersoff form [$E_2(6)$].

VI. CONCLUSION

We have used molecular-dynamics techniques to study the energetics and shapes of giant fullerenes. The atomic forces and total energies were computed from the electronic structure, using two different tight-binding models (one empirical, the other *ab initio*). The solution of the electronic problem was obtained using a recently developed order- N method, which produces the solution with an effort that scales linearly with the size of the system, therefore allowing the calculation of systems with thousands of atoms. We have developed efficient techniques to apply these order- N methods to the specific problem of large fullerenes, by using two different cutoff distances for the σ and π wave functions. This reduces the computational time, while maintaining an excellent accuracy. The results of our simulations show that, for large spherical clusters, the polyhedrally faceted shape is preferred, both for the empirical and for the *ab initio* calculations. These results contradict recent claims^{10,11} that isolated clusters may have rather spherical shapes, and rule out the possibility of an intrinsic stability of the spherical shape

in single-shell clusters as the cause of the observed sphericity of multisheet fullerenes. We have also shown that the spherical cage clusters have lower energy than toroidal cage clusters of the same size. However, the toroidal C_{360} and larger clusters have larger cohesive energies than the fullerene C_{60} and they are energetically stable. We also have studied the detailed way in which the energy of the spherical fullerenes approaches that of monolayer graphite when the size of the cluster is increased and used our computed energies to test several functional forms proposed in the literature.

ACKNOWLEDGMENTS

One of us (S.I.) acknowledges funding from Hitachi, Ltd. and would like to thank Dr. Sugie and Dr. Ihara for their encouragement. This work was partially supported by the NSF under Contracts Nos. DMR-89-20538 and DMR-93-22412, and by DOE Grant No. DEFG 02-91ER45439. Some of the computations were performed in the Convex C-3880 at the NCSA.

*Present address: Departamento de Física, Universidad de Oviedo (Spain).

¹H. W. Kroto, J. R. Heath, S. C. O'Brien, R. F. Curl, and R. E. Smalley, *Nature* (London) **318**, 162 (1985); W. Krätschmer, L. D. Lamb, K. Fostiropoulos, and D. R. Huffman, *ibid.* **347**, 354 (1990).

²See the collection of review articles published in *MRS Bull.* **XIX**, 11 (1994).

³D. Ugarte, *Nature* (London) **359**, 707 (1992); *Europhys. Lett.* **22**, 45 (1993).

⁴S. Iijima and T. Ichihashi, *Nature* (London) **363**, 603 (1993); **364**, 737(E) (1993); D. S. Bethune, C. H. Klang, M. S. de Vries, G. Gorman, R. Savoy, J. Vazquez, and R. Beyers, *ibid.* **363**, 605 (1993).

⁵A. M. Rao, P. Zhou, K.-A. Wang, G. T. Hanger, J. M. Holden, Y. Wang, W.-T. Lee, X.-X. Bi, P. C. Eklund, D. S. Cornett, M. A. Duncan, and I. J. Amster, *Science* **259**, 955 (1993).

⁶J. Tersoff, *Phys. Rev. B* **46**, 15 546 (1992).

⁷T. A. Witten and H. Li, *Europhys. Lett.* **23**, 51 (1993).

⁸M. Yoshida and E. Osawa, *Fullerene Sci. Tech.* **1**, 55 (1993).

⁹A. Maiti, C. J. Brabec, and J. Bernholc, *Phys. Rev. Lett.* **70**, 3023 (1993).

¹⁰D. York, J. P. Lu, and W. Yang, *Phys. Rev. B* **49**, 8526 (1994).

¹¹J. P. Lu and W. Yang, *Phys. Rev. B* **49**, 11 421 (1994).

¹²D. Ugarte, *MRS Bull.* **XIX**, 39 (1993).

¹³G. B. Adams, O. F. Sankey, M. O'Keefe, J. B. Page, and D. A. Drabold, *Science* **256**, 1792 (1992).

¹⁴P. Ordejón, D. A. Drabold, R. M. Martin, and M. P. Grumbach, *Phys. Rev. B* **51**, 1456 (1995), and references therein.

¹⁵P. Ordejón, D. A. Drabold, M. P. Grumbach, and R. M. Martin, *Phys. Rev. B* **48**, 14 646 (1993).

¹⁶F. Mauri, G. Galli, and R. Car, *Phys. Rev. B* **47**, 9973 (1993).

¹⁷W. Kohn, *Phys. Rev.* **115**, 809 (1959).

¹⁸C. H. Xu, C. Z. Wang, C. T. Chan, and K. M. Ho, *J. Phys. Condens. Matter* **4**, 6047 (1992); C. Z. Wang, C. T. Chan, and K.

M. Ho, *Phys. Rev. B* **46**, 9761 (1992).

¹⁹O. F. Sankey and D. J. Niklewski, *Phys. Rev. B* **40**, 3979 (1989)

²⁰F. H. Stillinger and T. A. Weber, *Phys. Rev. B* **31**, 5262 (1985); **33**, 1451(E) (1986).

²¹In the case of the spherical C_{2160} and C_{3840} , the tolerance in the maximum force was reduced to 0.02 eV/Å. A uniform expansion or contraction of a large fullerene produces small atomic forces, because the stress is distributed over the surface of the sphere, with a very small strain on each bond. Therefore, smaller tolerances in the forces are required for larger clusters.

²²Q. Zhang, J. -Y. Yi, and J. Bernholc, *Phys. Rev. Lett.* **66**, 2633 (1991).

²³C. S. Yannoni, P. P. Bernier, D. S. Bethune, G. Meijer, and J. R. Salem, *J. Am. Chem. Soc.* **113**, 3190 (1991).

²⁴B. I. Dunlap, D. W. Brenner, J. W. Mintmire, R. C. Mowrey, and C. T. White, *J. Phys. Chem.* **95**, 8737 (1991).

²⁵G. B. Adams (unpublished).

²⁶W. Yang, *Phys. Rev. Lett.* **66**, 1438 (1991).

²⁷S. Itoh, S. Ihara, and J. Kitakami, *Phys. Rev. B* **47**, 1703 (1993).

²⁸S. Ihara, S. Itoh, and J. Kitakami, *Phys. Rev. B* **47**, 12 908 (1993).

²⁹S. Itoh and S. Ihara, *Phys. Rev. B* **48**, 8323 (1993).

³⁰F. F. Abraham and I. P. Batra, *Surf. Sci.* **209**, L125 (1989).

³¹S. Iijima, P. M. Ajayan, and T. Ichihashi, *Phys. Rev. Lett.* **69**, 3100 (1992); M. Endo (private communication).

³²S. Itoh and P. Ordejón (unpublished).

³³J. K. Johnson, B. N. Davidson, M. R. Pederson, and J. Q. Broughton, *Phys. Rev. B* **50**, 17 575 (1994).

³⁴J. C. Greer, S. Itoh, and S. Ihara, *Chem. Phys. Lett.* **222**, 621 (1994).

³⁵J. Tersoff, *Phys. Rev. B* **37**, 6991 (1988).

³⁶W.H. Press *et al.*, *Numerical Recipes, The Art of Scientific Computing* (Cambridge University Press, Cambridge, England, 1986).

³⁷G. L. Bretthorst, *Bayesian Spectrum Analysis and Parameter Estimation* (Springer-Verlag, Berlin, 1988), Chap. 5.